

Nanoscale Chemical Imaging of *Bacillus Subtilis* Spores by Combining Tip-Enhanced Raman Scattering and Advanced Statistical Tools (Supporting Information)

Giulia Rusciano,^{*,†} Gianluigi Zito,[†] Rachele Isticato,[‡] Teja Sirec,[‡] Ezio Ricca,[‡]
Elena Bailo,[¶] and Antonio Sasso[†]

Department of Physics, University of Naples Federico II, via Cintia, 80126-I Naples, Italy,
Department of Biology, University of Naples Federico II, via Cintia, 80126-I Naples, Italy,
and WITec GmbH, Lise-Meitner-Str. 6, DE-89081 Ulm, Germany

E-mail: giulia.rusciano@unina.it

Insight on spore architecture

Wild-type *B. Subtilis* spores are often considered as a model system for spore-forming bacteria. They exhibit a roughly ellipsoidal shape, with the short axis $\sim 0.6 \mu\text{m}$ and the long axis $\sim 1.3 \mu\text{m}$ (average values). The peculiar structure of the spore is characterized by several protective layers surrounding a dehydrated cytoplasm and is responsible of the extreme resistance of the spore to external physical and chemical insults.^{1,2} The core, the

^{*}To whom correspondence should be addressed

[†]University of Napoli Federico II

[‡]University of Napoli Federico II

[¶]WITec GmbH

innermost part of the spore, contains the cytoplasm with proteins, stable RNAs and DNA. The core cytoplasm is dehydrated and has a water content of only 30-50%, as opposed to the 70-90% typical of vegetative cell cytoplasm. Within the core is also highly abundant the spore-specific compound pyridine-2,6-dicarboxylic acid (dipicolinic acid, DPA) which accounts for about 15% of the total spore weight and forms complexes with divalent cations, mainly Ca^{2+} (CaDPA). DPA plays an important role in spore resistance to wet heat and UV irradiation. The cortex, a thick peptidoglycan-like layer, surrounds the inner membrane and is essential for maintenance of the dehydrated state of the core and contributes to thermal resistance and dormancy. Outside of the cortex is the coat, a ~ 50 nm thick proteinaceous structure organized in a lamellar inner fraction and an electron-dense outer layer. More than 70 different proteins, about 10% of the spore dry weight, form the coat, whose function is to protect the spore from toxic chemicals and lytic enzymes. Recently an additional coat layer has been observed and named crust. In addition to structural proteins, the coat is also composed of polysaccharides which modulate the relative hydrophobicity of the spore. At present not many details are available about the precise glycan composition of the spore surface.

Experimental set-up

The following figure reports a scheme of our TERS set-up.

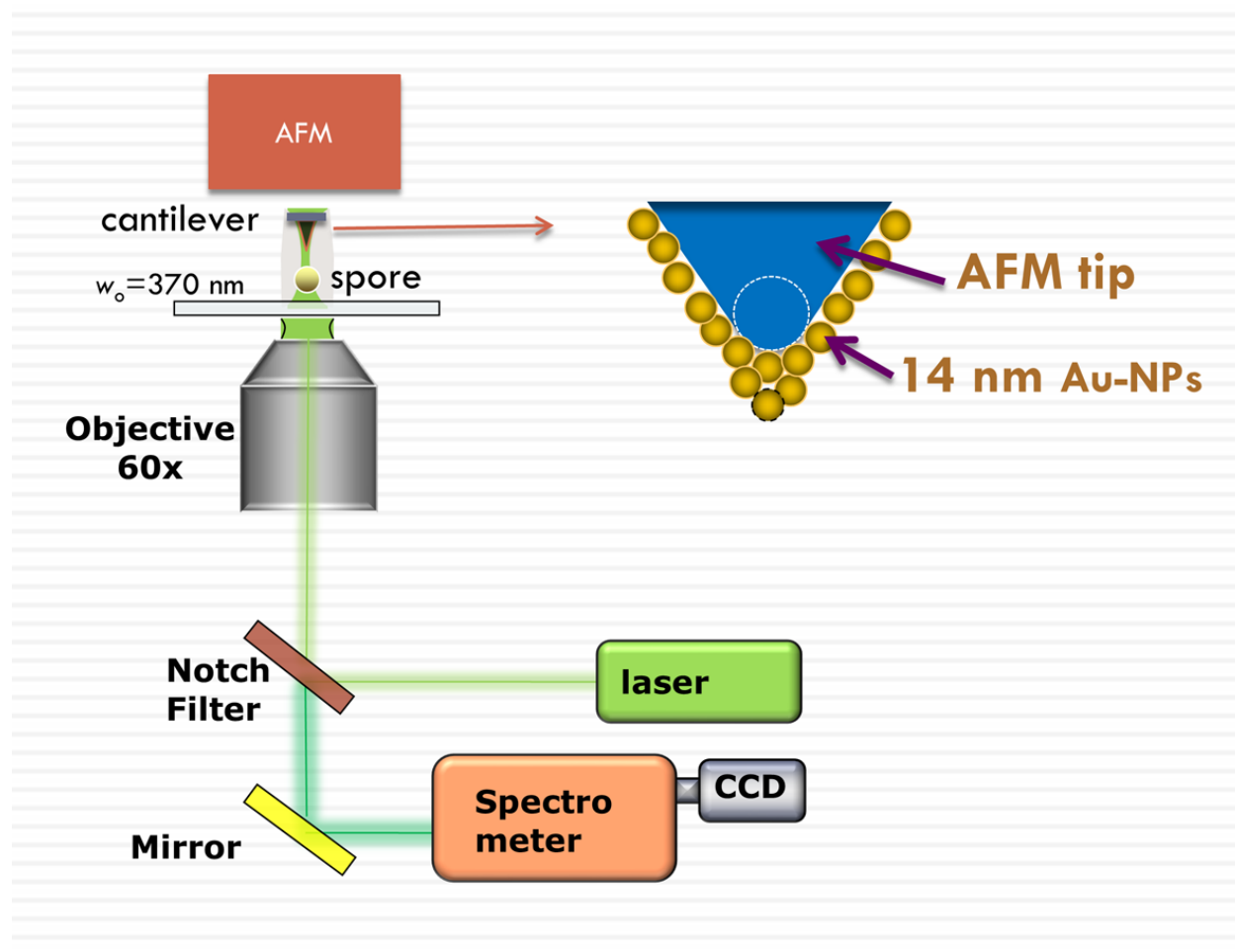


Figure S1: Schematic picture of our TERS set-up. A cartoon of the TERS tips used in this work is also reported.

Statistical analysis of TERS maps from CNTs on glass

Prior to testing our BC- and PCA-based approaches with spores, we tested them on a much more simple sample, consisting in CNT-bundles pipetted on a glass coverslip. Figure S2a reports the AFM topography of a $10\mu\text{m} \times 10\mu\text{m}$ film area. Single-point TERS spectra are depicted in Figure S2b. The analysis of TERS spectra acquired during the same sample scan was initially performed by following the simple approach, often reported in literature,^{3,4} based on the construction of TERS maps from the strength of selected peaks, as shown in Figure S2c. This approach was quite successful in reconstructing almost all the features of the acquired map. As an obvious consequence, also applying more sophisticated tools for TERS imaging analysis gave a straightforward correspondence with the AFM map. For instance, for the application of BA, we naturally recognized as basis functions the more representative single-point spectra acquired in particular positions of the sample and shown in Figure S2b. The results of this analysis are shown in Figure S2d where the corresponding Basis Component (BC) maps are depicted. The features reconstructed in BC maps clearly correspond to the specific spectral features highlighted in the intensity maps of Figure S2c. For instance, the map associated to the basis function 2, *i.e.* corresponding to the spectrum of a CNT with a ring breathing mode at 278 cm^{-1} , basically matches the intensity map reporting the strength of the peak at 278 cm^{-1} , depicted in Figure S2c. More interesting is the application of PCA, due to the unbiased character of this analysis. However, even this analysis reports the same information, and the score maps of the first four principal components (PCs) mirrors that obtained by BA (Figure S2e). Moreover, the PC loading exhibit spectral features quite similar to the spectra selected as basis functions (data not shown). Therefore, it is clear that when sample exhibits quite well identifiable and characteristic spectral features and, moreover, it is placed in a quite homogeneous and weakly scattering medium (as water), the spectra analysis is straightforward and clear correlations with AFM-maps can be immediately found.

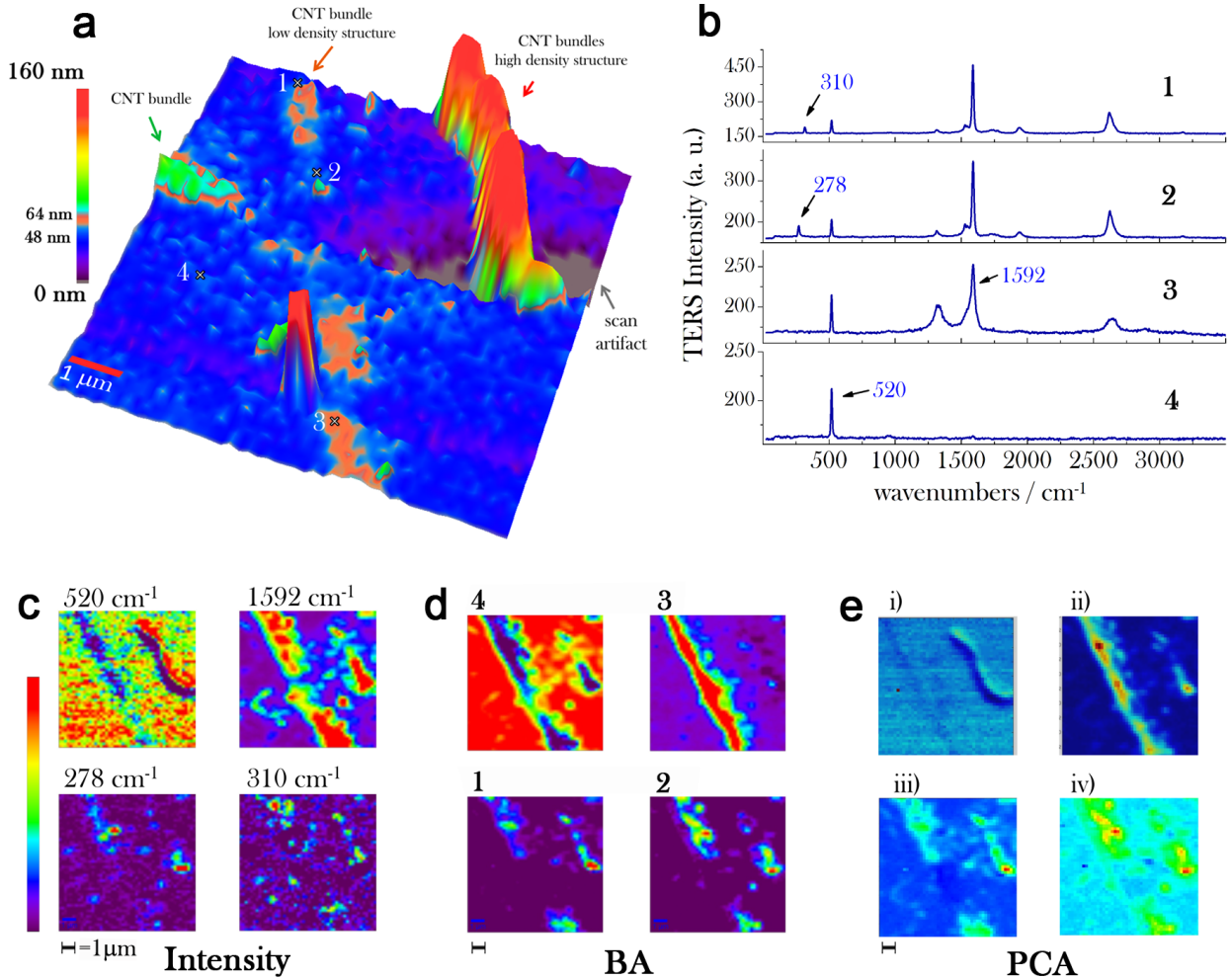


Figure S2: **a**, AFM-height map of CNT-bundles pipetted on a glass coverslip. **b**, Selected spectra corresponding to the points indicated in **a** by white crosses. Spectra 1 and 2 represent the signals from two different CNT types, as inferred by the presence of ring breathing modes with a different shift; spectrum 3 is probably due to a CNT bundle in the sample; spectrum 4 represents the spectra acquired in a clean part of the scanned region, therefore it exhibits only the feature at 520 cm⁻¹, due to the bulk Si of the TERS tip. **c**, TERS maps obtained by reporting the intensity of selected peaks (520, 1530, 310 and 278 cm⁻¹), as indicated in the map-labels. **d**, Basis Component (BC) maps resulting from the application of BA to the acquired TERS data set decomposed along spectra 1-4 of **b** used as basis spectra. **e**, Score maps resulting from the application of PCA to TERS spectra: maps in (i), (ii), (iii) and (iv) correspond to the first four principal component (PC) maps of the TERS data scan.

TERS spectra

In Figure S3, we show the TERS spectra acquired in the raster scanning analyzed in Figure 3 of the main manuscript.

Images Correlation Analysis

To evaluate quantitatively the correlation between AFM-phase image and TERS maps, we calculated the Pearson coefficient,⁵ defined by the relation:

$$P = \frac{\sum_m \sum_n (A_{nm} - \bar{A})(B_{nm} - \bar{B})}{\sqrt{(\sum_m \sum_n (A_{nm} - \bar{A})^2)(\sum_m \sum_n (B_{nm} - \bar{B})^2)}} \quad (1)$$

being A_{nm} (B_{nm}) the pixel intensity matrix of the first (second) image and \bar{A} (\bar{B}) its mean value. This analysis has been done by using subroutines available in Matlab environment. In Figure S4 we report both the AFM-phase image (S4a) and the TERS maps (S4b-d) obtained across a ridge. In particular, maps shown in S4b report the intensity of selected bands (highlighted in the map labels), while maps in S4c and S4d result from the statistical analysis of TERS data by BA and PCA, respectively. For BA, basis functions correspond to the average spectra of points on the ridge (zone 1) and out of the ridge (zone 2). Table S1 reports the Pearson coefficient evaluated for all these maps. As it is possible to see, a clear correlation is demonstrated for the PCA-based maps and, to a lesser extent, to BA-based maps, confirming the results shown in the paper. Note that the Pearson coefficients BC2-component map is negative, as a consequence of the fact that BC2 components is more present in zone 2 (out of the ridge). Figure S5 reports the same maps shown in Fig. S4, but acquired in a phase-uniform region. In this case, BA was performed by assuming as basis functions the average spectra from two arbitrary selected regions, highlighted in the phase map by rectangles. As it is possible to see, in this case no significant clustering of pixel can be appreciated, meaning that both BA- and PCA-based approaches do not *see*

the presence of homogeneous sub-regions. Moreover, the statistical analysis of TERS data does not suggest any correlation with the AFM-phase map, although the Pearson coefficient is somewhat higher for maps resulting from the statistical analysis of TERS spectra (Table S2).

Table 1: Pearson correlation coefficient between the AFM-phase map shown in Fig. S3a and the spectroscopic (Fig. 3Sb) TERS maps, as well as the maps obtained by statistical analysis of TERS data (S3c-d).

<i>Pearson coefficients</i>						
Intensity maps			BA maps		PCA maps	
I_{830}	I_{930}	I_{1570}	BC1-map	BC2-map	PC2-map	PC3-map
0.10	-0.11	-0.09	0.59	-0.79	0.86	0.79

Table 2: Pearson correlation coefficient between the AFM-phase map shown in Fig. S4a and the spectroscopic (Fig. S4b) TERS maps, as well as the maps obtained by statistical analysis of TERS data (S4c-d).

<i>Pearson coefficients</i>						
Intensity maps			BA maps		PCA maps	
I_{830}	I_{930}	I_{1570}	BC1-map	BC2-map	PC2-map	PC3-map
0.08	-0.03	-0.10	0.11	0.12	-0.26	0.12

References

1. McKenney, P. T.; Driks, A.; Eichenberger P. The Bacillus subtilis spore: assembly and functions of the multilayered coat. *Nat. Rev. Microbiol.* **2013**, *11*, 33-44.
2. Plomp, M.; Carroll, A.M.; Setlow, P.; Malkin, A.J. Architecture and Assembly of the Bacillus subtilis Spore Coat. *PLoS ONE* **2014**, *9*, e108560-e108575.
3. Stadler, J.; Schmid, T.; Zenobi, R. Nanoscale Chemical Imaging Using Top-Illumination Tip-Enhanced Raman Spectroscopy. *Nano Lett.* **2010**, *10*, 4514-4520.
4. Stadler, J.; Schmid, T.; Opilik, L.; Kuhn, P.; Dittrich, P.; Zenobi, R. Tip-enhanced Raman Spectroscopic Imaging of Patterned Thiol Monolayers. *Beilstein. J. Nanotechnol.* **2011**, *2*, 509-515.

5. Rodgers, J.L.; Nicewander, W.A. Thirteen ways to look at the correlation coefficient
Amer. Statist. **1995** *42*, 59-66.

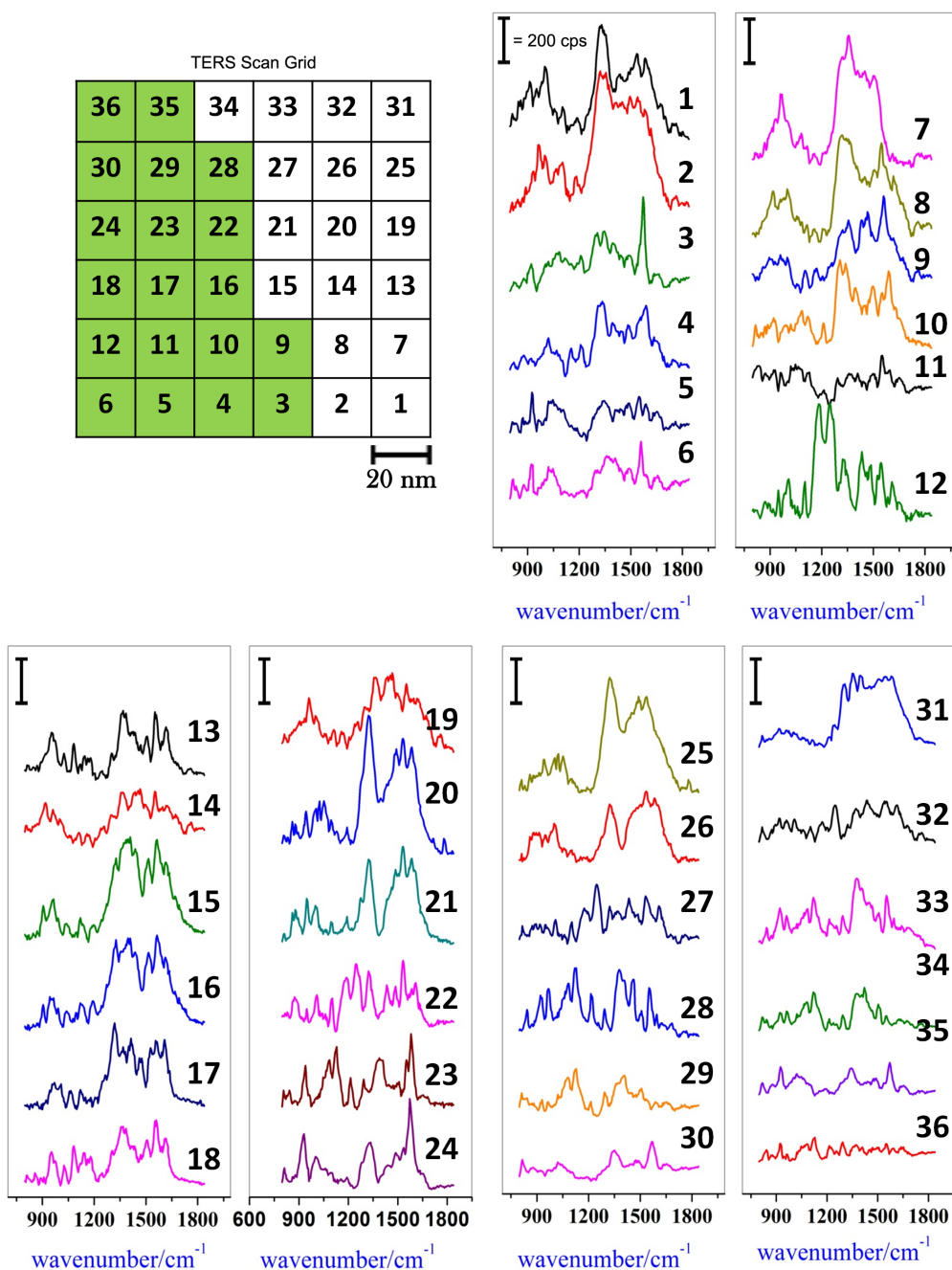


Figure S3: Detailed TERS spectra acquired in the 120 nm × 120 nm raster scan shown in Figure 3 of the paper. The number close to each spectrum indicates the position on which it was acquired (see the raster scanning scheme in the upper part of the figure): green pixels correspond to zone 1; white pixels correspond to zone 2 of Figure 3 (phase map).

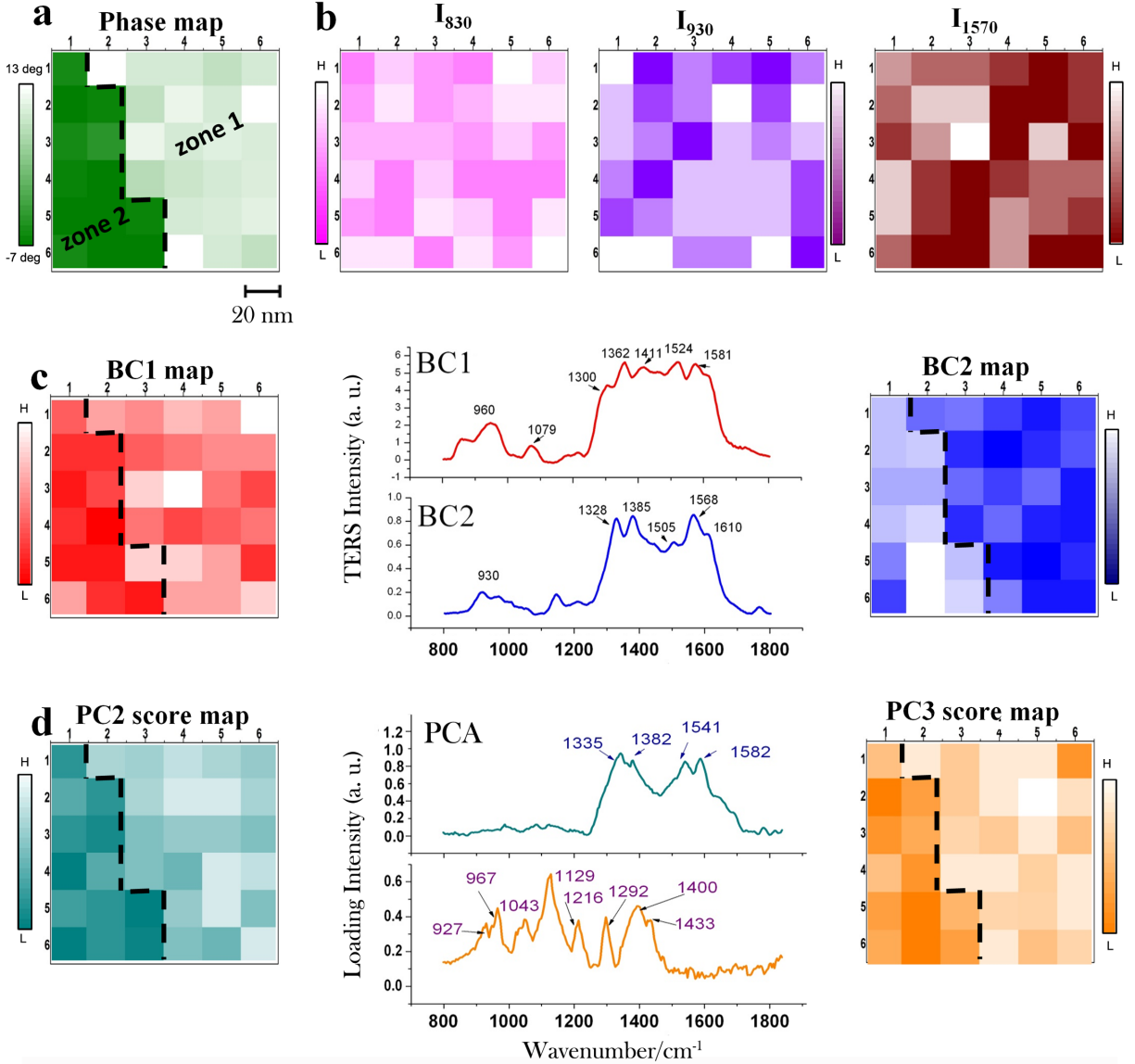


Figure S4: **a**, AFM-phase map across a ridge of a *B. Subtilis* spore. Zone 1 corresponds to the ridge. **b**, TERS maps obtained by reporting the intensity of assigned spectral features, indicated in the map labels. **c**, BC1- and BC2-maps (sides), calculated by projecting each spectrum on BC1 and BC2 components, shown in the central part. **d**, PC2- and PC3-score maps (sides) and loadings (central part). Scale bar=20 nm. Color bar: L=low level, H=high level.

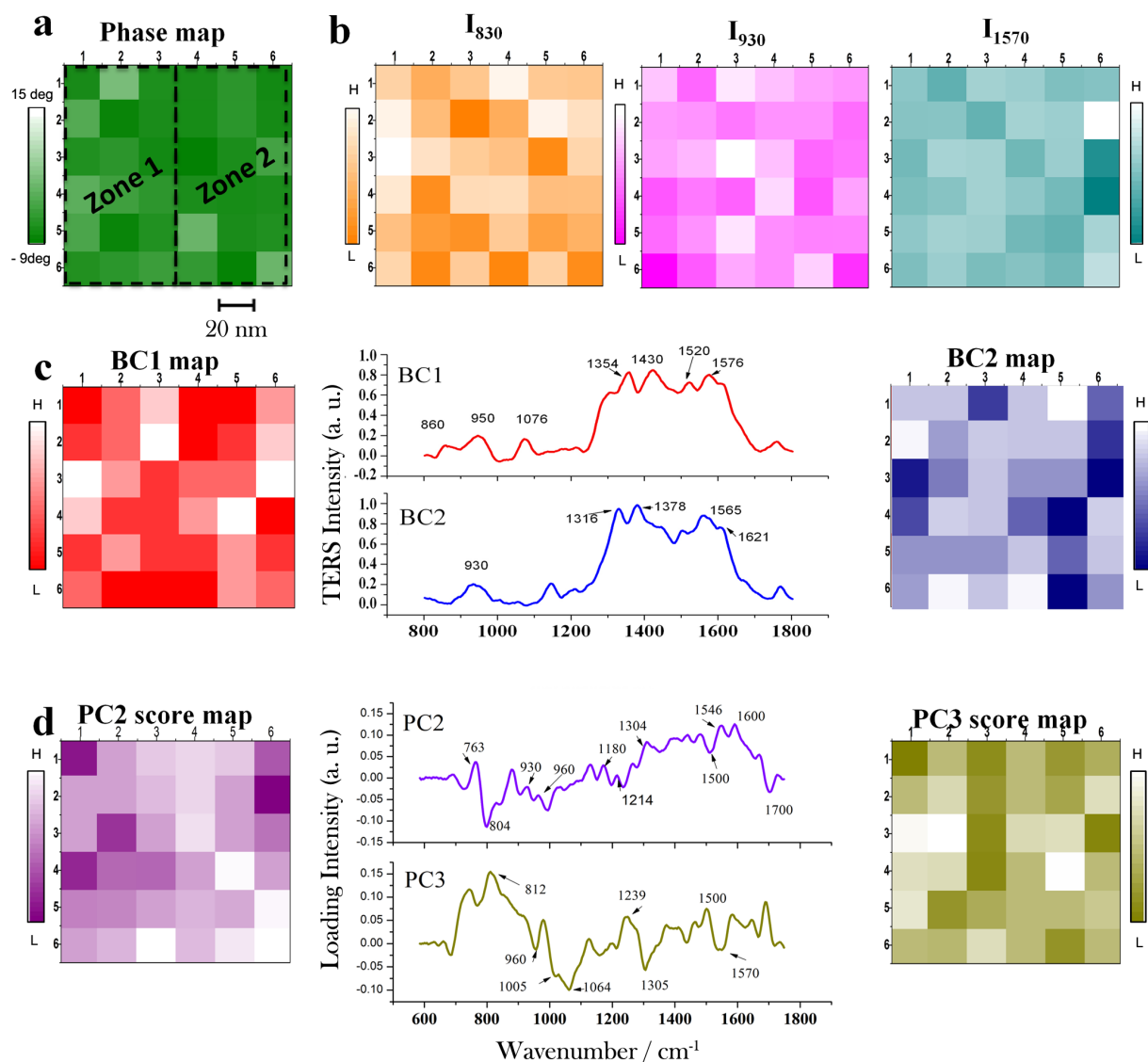


Figure S5: **a**, AFM-phase map of a *B. Subtilis* surface, in a *homogeneous* phase region (not across a ridge). **b**, TERS maps obtained by reporting the intensity of assigned spectral features, indicated in the map labels. **c**, BC1- and BC2-maps (sides), calculated by projecting each spectrum on BC1 and BC2 components, shown in the central part. BC1 and BC2 components correspond to the average spectra calculated in the two regions defined by the rectangles in part a. **d**, PC2- and PC3-score maps (sides) and loadings (central part). Scale bar=20 nm. Color bar: L=low level, H=high level.